PAPER

Temperature dependence of spin–orbit torques in Pt/Co/Pt multilayers

IOP Publishing Journal of Physics D: Applied Physics
J. Phys. D: Appl. Phys. **51** (2018) 095001 (6pp) https://doi.org/10.1088/1361-6463/aaa7c8

Temperature dependence of spin–orbit torques in Pt/Co/Pt multilayers

Shiwei Chen, Dong Li, Baoshan Cui, Li Xi, Mingsu Si, Dezheng Yang[1] and Desheng Xue[1]

Key Laboratory for Magnetism and Magnetic Materials of Ministry of Education, Lanzhou University, Lanzhou 730000, People's Republic of China

E-mail: yangdzh@lzu.edu.cn and xueds@lzu.edu.cn

Received 24 October 2017, revised 7 December 2017
Accepted for publication 15 January 2018
Published 9 February 2018

Abstract

We studied the current-induced spin–orbit torques in a perpendicularly magnetized Pt (1 nm)/Co (0.8 nm)/Pt (5 nm) heterojunction by harmonic Hall voltage measurements. Owing to similar Pt/Co/Pt interfaces, the spin–orbit torques originated from the Rashba effect are reduced, but the contribution from the spin Hall effect is still retained because of asymmetrical Pt thicknesses. When the temperature increases from 50 to 300 K, two orthogonal components of the effective field, induced by spin–orbit torques, reveal opposite temperature dependencies: the field-like term (transverse effective field) decreases from 2.3 to 2.1 (10^{-6} Oe (A cm^{-2})$^{-1}$), whereas the damping-like term (longitudinal effective field) increases from 3.7 to 4.8 (10^{-6} Oe (A cm^{-2})$^{-1}$). It is noticed that the damping-like term, usually smaller than the field-like term in the similar Pt/Co interfaces, is twice as large as the field-like term. As a result, the damping-like spin–orbit torque reaches an efficiency of 0.15 at 300 K. Such a temperature-dependent damping-like term in a Pt/Co/Pt heterojunction can efficiently reduce the switching current density which is 2.30×10^6 A cm^{-2} at 300 K, providing an opportunity to further improve and understand spin–orbit torques induced by spin Hall effect.

Keywords: spin–orbit torques, perpendicular magnetic anisotropy, current induced magnetization switching, temperature dependence

(Some figures may appear in colour only in the online journal)

1. Introduction

Spin–orbit torques (SOTs) in ferromagnetic metal (FM)/nonmagnetic heavy metal (NM) heterojunctions induced by in-plane currents have attracted robust research interests, and they have been demonstrated as an alternative approach to switch the magnetization efficiently [1, 2], to drive fast chirality dependent domain wall motion [3–5], as well as to excite high-frequency magnetization oscillations [6–8]. Generally, two sorts of spin–orbit coupling (SOC) mechanisms have been considered as candidate sources for SOTs: the spin current can be generated in the NM layer with the bulk spin Hall effect (SHE) [9], which can diffuse into the adjacent FM layer and exert torques on the moments via spin transfer torque [10]. On the other hand, SOTs can also be induced from the interfacial Rashba effect [11], for which the accumulated spins at the interface can force the moments to change their direction by direct exchange coupling [12].

Generally speaking, most of investigations focus on two orthogonal SOTs, namely the damping-like torque with the form of $\boldsymbol{\tau}_D \propto \boldsymbol{m} \times (\boldsymbol{\sigma} \times \boldsymbol{m})$ and the field-like torque with the form of $\boldsymbol{\tau}_F \propto \boldsymbol{m} \times \boldsymbol{\sigma}$, where $\boldsymbol{m}$ and $\boldsymbol{\sigma}$ are unit vectors of the magnetization in the FM layer and spin polarization direction in the NM layer, respectively. For ferromagnetic materials, the damping-like torque can overcome the magnetization damping, and switch the magnetic moments directly [13]. The field-like torque can lower the energy barrier of switching, and affect the magnetic dynamic processes [14]. More interestingly, it is reported that these two SOTs are used to rotate the antiferromagnetic moments that are immune to magnetic

[1] Authors to whom any correspondence should be addressed.

field due to the net zero magnetization [15]. Therefore, tuning these two kinds of SOTs is the key for practical use of SOTs in spintronic devices.

Nowadays, these two kinds of SOTs in FM/NM heterojunctions have been widely studied through using various methods, such as varying the thicknesses of FM and NM layers [16], modulating the chemical ordering [17], inserting additional metal and oxidation layers [18, 19], and changing the structure of the stacks [20]. However, the investigations on the temperature feature of SOTs are controversial and the underlying physics is unclear. For the Ta/CoFeB/MgO system, Qiu *et al* found that the field-like torque increased with decreasing temperature, whereas the damping-like torque was insensitive to temperature [21]. Similar results were also confirmed by Kim *et al* [22]. By varying Ta thicknesses, Kim *et al* further separated the temperature-dependent SOTs into the interface (i.e. Rashba effect) and the bulk effect (i.e. SHE), where the Rashba effect was unchanged with temperature, and SHE dominated the temperature feature of SOTs. In the case of NM/FM/oxide asymmetrical heterojunctions, Ou *et al* [23] inserted the Hf and HfO_x into the interfaces of NM/FM and FM/oxidation, respectively. They found that the field-like torque was yielded by the spin scattering at interfaces due to the spin current in NM via SHE, rather than the Rashba effect. Moreover, a different temperature dependence of SOTs was reported in weak spin–orbit coupling $Cu_{40}Au_{60}$ metal, where the damping-like torque increased with temperature, but the filed-like torque decreased with temperature [24]. As mentioned above, the asymmetrical structure was used to enhance the efficiency of the SOTs. This makes it difficult to quantitatively separate the temperature-dependencies of these two SOTs, because the Rashba effect and SHE are mixed in those asymmetrical heterojunctions. Thus, to study the origins of temperature-dependent SOTs is necessary.

In this work, we used a Pt/Co/Pt heterojunction to study the temperature dependence of SOTs. The magnitude and orientation of the field-like and the damping-like torques were measured by the harmonic Hall voltage measurements [25]. In contrast to the fact that the field-like torque is larger than the damping-like torque in the asymmetrical heterojunction, the field-like torque is two times less than the damping-like torque in our Pt/Co/Pt heterojunction. At 300 K, the field-like torque is only 2.1×10^{-6} Oe $(\text{A cm}^{-2})^{-1}$ and the damping-like torque reaches 4.8×10^{-6} Oe $(\text{A cm}^{-2})^{-1}$. This means that the Rashba effect is reduced compared with the asymmetrical Ta/CoFeB/MgO heterojunction [23] due to the similar Pt/Co/Pt interfaces, as expected. More interestingly, since SHE dominates SOTs in our experiment, the damping-like torque with respect to SHE contrasts with the previous temperature independence feature. With increasing the temperature from 50 to 300 K, the damping-like torque increases from 3.7×10^{-6} Oe $(\text{A cm}^{-2})^{-1}$ to 4.8×10^{-6} Oe $(\text{A cm}^{-2})^{-1}$. At 300 K, the damping-like spin–orbit torque efficiency can reach up to 0.15, which yields the switching current as low as 2.30×10^6 A cm^{-2}. These results provide potential applications at high temperature for the Pt/Co/Pt heterojunction and are helpful to further understand the origins of SOTs.

2. Experiment

The film stack of Ta(3)/Pt(5)/Co(0.8)/Pt(1)/AlO_x(2) (thickness in nanometers) was deposited on Corning glass substrate by magnetron sputtering with a base pressure 4.0×10^{-5} Pa. The film was patterned into 8.9 μm wide and 190 μm length Hall bars using standard lithography and Ar-ion milling techniques. Figure 1(a) displays a schematic of the sample layout and the measurement configuration. When the in-plane current is applied along the $+x$ direction, the spin current in the top and bottom Pt layers diffuses into the Co layer with inverse spin polarization due to SHE. Owing to asymmetrical Pt thicknesses, the net spin current, which exerts SOTs on the Co magnetization, can be obtained, as shown in the zoom-in area of figure 1(a). In figure 1(b), the anomalous Hall effect (AHE) curves were measured under the magnetic field H_{ext} along the z axis. The sharp switching of AHE resistance (R_{H}) indicates a good perpendicular magnetic anisotropy of the Co layer in the temperature range from 50 to 300 K. Figure 1(c) shows the AHE curves when H_{ext} is swept along the x axis. It clearly shows that R_{H} decreases with increasing H_{ext}, indicating that the magnetization of Co is gradually rotated from out-plane to in-plane.

Owing to exerting SOTs on the Co layers, the current-induced magnetization switching is realized, as shown in figures 1(d) and (e). In order to break the symmetry of magnetization switching in response to the SOTs, we applied a fixed external magnetic field along the x direction. One can easily find that the magnetization switching, induced by current, shows a typical hysteresis loop, but the switching direction depends on the sign of the external magnetic field. For a positive magnetic field $H_{\text{ext}} = +500$ Oe, the switching direction is clockwise, as shown in figure 1(d). However, for a negative magnetic field, $H_{\text{ext}} = -500$ Oe, the switching direction is anticlockwise, as shown in figure 1(e). The switching direction dependence of H_{ext} can be well understood in the term of the macro spin model [2]. Remarkably, in our Pt/Co/Pt heterojunction, the switching current density is around 2.30×10^6 A cm^{-2} at 300 K, which is very close to the value observed in the asymmetrical heterojunction Pt/Co/Ta with an inverse spin Hall angle of Pt and Ta [26].

In order to further quantitatively measure the magnitude of the effective field (H_{DL} and H_{FL}) induced by SOTs, the harmonic Hall voltage measurements were taken [25]. A sinusoidal current ($I = I_0 \sin \omega t$) with a frequency of 133 Hz was applied through the Hall bars along the x axis, then we measured the first ($V_{1\omega}$) and the second ($V_{2\omega}$) harmonic Hall voltages as a function of in-plane external fields using the AD/DA card, which reflect the Co magnetization oscillations driven by the external magnetic field and SOTs, respectively. As shown in figures 2(a) and (b), $V_{1\omega}$ shows similar parabolic behaviors both for H_x and H_y, respectively. However, $V_{2\omega}$ shows different linear behaviors for H_x and H_y, depending on the magnetic field direction with respect to the current flow direction (i.e. longitudinal or transverse magnetic field). For the longitudinal magnetic field in figure 2(c), the signs of slopes of $V_{2\omega}$ are the same for the magnetic states along $+z$ and $-z$ directions,

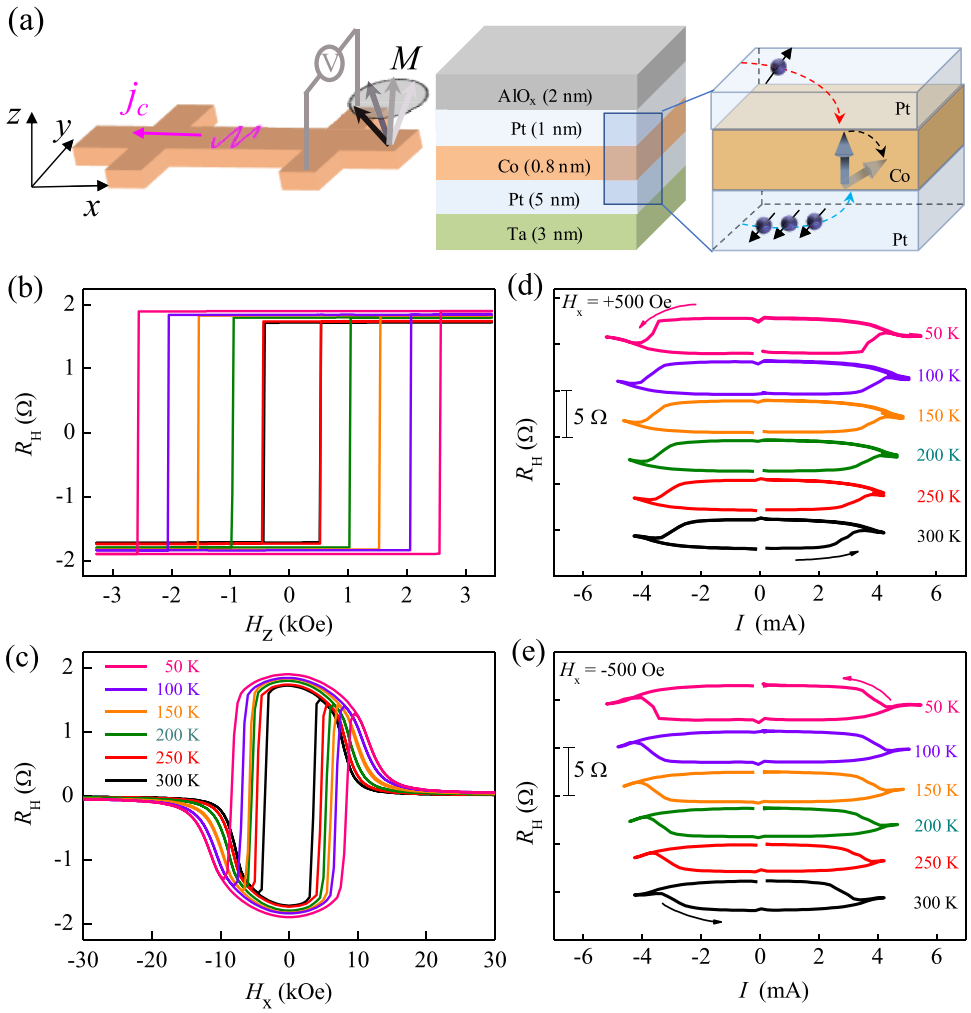

Figure 1. (a) Measurement configuration and schematic of a Ta/Pt/Co/Pt/AlO$_x$ multilayer. The zoomed-in area shows that spin current is injected from top and bottom Pt layers and then switches the Co magnetization. The measured R_H curves when H_{ext} is fixed in the (b) $+z$ direction and (c) $+x$ direction. Magnetization switching characterized by R_H for (d) $H_x = 500$ Oe and (e) $H_x = -500$ Oe when temperature is changed from 50 to 300 K.

whereas for the transverse magnetic field in figure 2(d), the signs of slopes are reversed for $\pm M_z$. This can be easily understood by considering that the longitudinal (transverse) component of SOTs has an even (odd) symmetry with respect to the inversion of the magnetization [27].

The damping-like effective field H_{DL} (longitudinal effective field) and field-like effective field H_{FL} (transverse effective field) can be calculated using the following relation [16]:

$$H^0_{DL(FL)} = -2\frac{\partial V_{2\omega}}{\partial H_{x(y)}} \Big/ \frac{\partial^2 V_\omega}{\partial H^2_{x(y)}}. \quad (1)$$

According to equation (1), the first and second harmonic curves were fitted through the quadratic and linear functions, respectively. To further consider the influence of planar Hall effect (PHE), the modified $H^1_{DL(FL)}$ can be determined by [25]:

$$H^1_{DL(FL)} = \frac{H^0_{DL(FL)} \pm 2rH^0_{FL(DL)}}{1 - 4r^2}, \quad (2)$$

where r is the ratio of PHE resistance (R_{PHE}) and AHE resistance (R_{AHE}) and the $\pm$ sign is the magnetization direction $\pm$Z. The angular dependence of Hall resistance R_H and the fitting curves in the temperature range of 50–300 K are shown in figure 3(a), where an in-plane magnetic field of 5 T is applied to saturate the magnetization. R_{PHE} is obtained by the fitting equation: $R_H = \frac{1}{2}R_{AHE}\cos\theta + \frac{1}{2}R_{PHE}\sin^2\theta\sin 2\varphi$. Here, the fitting parameter $\theta = 87°$ indicates a small misalignment between the sample plane and the applied magnetic field. The extracted ratio r in the temperature range of 50–300 K is shown in figure 3(b). H^1_{DL} and H^1_{FL} at 300 K are plotted as a function of current density j_c in figures 3(c) and (d), respectively. H^1_{DL} and H^1_{FL} are both linear with j_c, indicating that the Joule heating and other non-linear effects can be negligible. At 300 K, H^1_{DL} (β_{DL}) and H^1_{FL} (β_{FL}) per unit current density are 4.8×10^{-6} and 2.1×10^{-6} Oe (A cm^{-2})$^{-1}$, respectively. Although both the Rashba effect and SHE contribute two effective fields, the mechanisms behind them are different. The Rashba effect generally contributes a larger H_{FL} than H_{DL} by analyzing drift-diffusion [28], while SHE contributes a larger H_{DL} than H_{FL} due to the absorption of the transverse polarized spin current [23]. Interestingly, in our Pt/Co/Pt heterojunction, H_{DL} is twice as large as H_{FL}, which contrasts with the previous results of asymmetrical structure where H_{DL} is

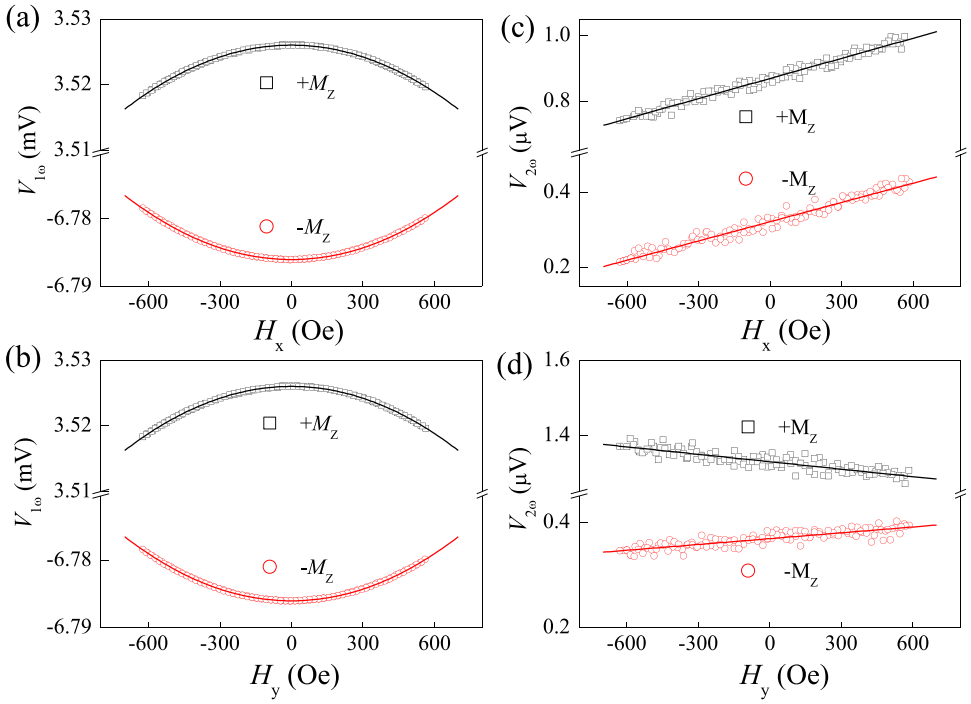

Figure 2. The first harmonic voltages $V_{1\omega}$ versus in-plane (a) longitudinal magnetic field H_x and (b) transverse magnetic field H_y at 300 K. The second harmonic voltages $V_{2\omega}$ versus in-plane (c) longitudinal magnetic field H_x and (d) transverse magnetic field H_y at 300 K. The hollow black and red symbols correspond to $+M_z$ and $-M_z$ magnetized states, respectively. The solid lines stand for the fitting results.

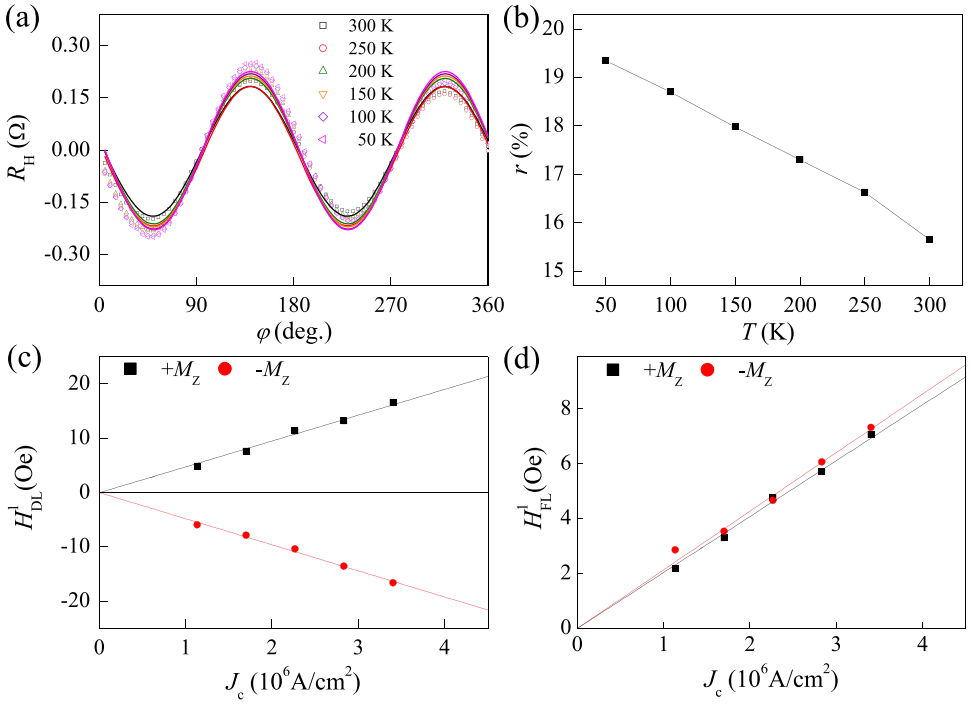

Figure 3. (a) Hall resistance R_H as a function of angle φ in the temperature range from 50 to 300 K. The solid line is a fit to obtain the planar Hall resistance R_{PHE}. (b) The correction factor r as a function of temperature from 50 to 300 K. (c) Damping-like effective field H^1_{DL} as a function of J_c at 300 K. (d) Field-like effective field H^1_{FL} as a function of J_c at 300 K.

usually much smaller than H_{FL} [21]. Thus, the Rashba effect is indeed reduced due to our Pt/Co/Pt heterojunction, in consistency with the previous work of the similar heterojunction Pt/Co/Pt [29].

In order to further study the origin of SOTs in Pt/Co/Pt heterojunction, the temperature dependences of H_{DL} and H_{FL} per unit current density ($\beta_{DL} = H_{DL}/J_c$ and $\beta_{FL} = H_{FL}/J_c$) are summarized in figures 4(a) and (b), respectively. The results

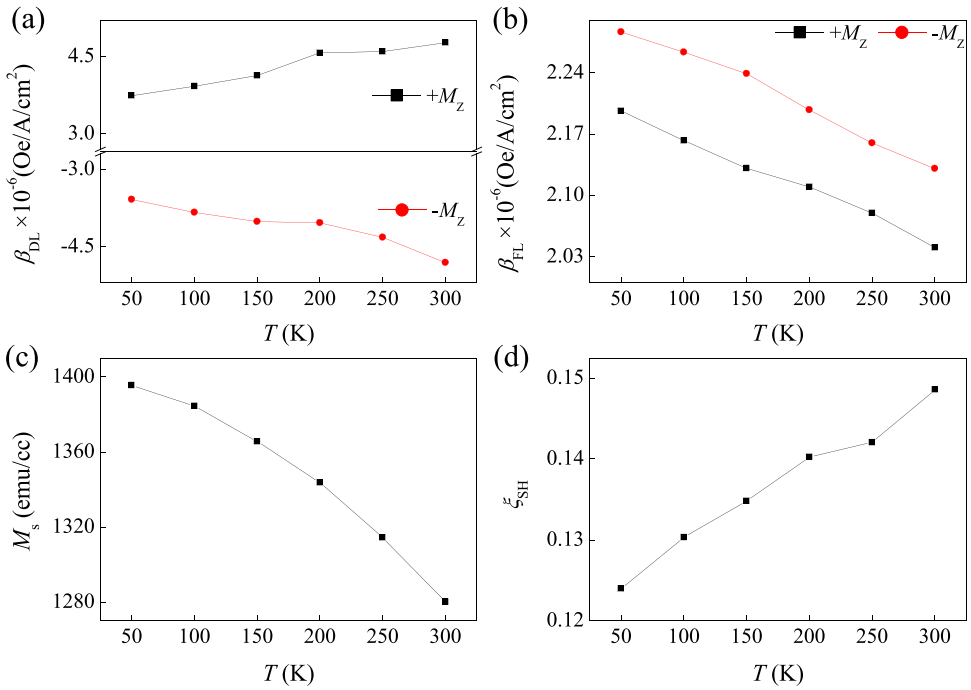

Figure 4. The temperature dependence of (a) β_{DL} (damping-like effective field per unit current density), (b) β_{FL} (field-like effective field per unit current density), (c) saturation magnetization of Co and (d) ξ_{SH} (spin Hall efficiency).

show that both types of SOTs are affected by the temperature, but present opposite behaviors. With increasing temperature, β_{DL} increases, but β_{FL} decreases. The opposite temperature dependence of β_{DL} and β_{FL} indicates two different underlying mechanisms. Owing to the similar Pt/Co/Pt interface, the Rashba effect is reduced. Given that the damping-like torque originates from the SHE, the relation between H_{DL} and effective SOTs efficiencies ξ_{SH} is given by $\xi_{SH} = J_s/J_c = 2|e|M_s t_F H_{DL}/(\hbar J_c)$, where e is the elementary charge, t_F is the thickness of the ferromagnetic layer, $\hbar$ is the reduced Planck constant, and M_s is the saturation magnetization of Cobalt (figure 4(c)). Figure 4(d) shows that the effective SOTs efficiencies ξ_{SH} increase with the increasing temperature. The value of ξ_{SH} is around 0.15 at 300 K, which is consistent with the reported value of 0.06–0.19 [12, 30–32]. The damping-like torque not only depends on the spin Hall torque efficiency (ξ_{SH}), but also is affected by the saturation magnetization (M_s). In the framework of the SHE, which is considered as the main source of the damping-like torque and of the conventional spin transfer theory in ferromagnets, the damping-like effective field H_{DL} is usually described by the formula [33]:

$$\frac{H_{DL}}{j_c} = \frac{\hbar}{2|e|t_F}\frac{1}{M_s}\xi_{SH}. \quad (3)$$

In Pt/GdFeCo bilayers, owing to the strong temperature-dependent M_s from ferrimagnet GdFeCo, H_{DL}/J_c and $1/M_s$ have been confirmed to have a nice linear relationship [34]. Because in our results M_s decreases with increasing the temperature, it is necessary to distinguish the contributions of $1/M_s$ and ξ_{SH} to the damping-like effective field H_{DL}. When the temperature increases from 50 to 300 K, the relative variation ratio of H_{DL}/J_c reaches 27.37%, but $1/M_s$ is only increased to 9.01%. This indicates that the increasing of ξ_{SH} plays a dominant role for the temperature dependence on the damping-like effective field.

The fact that ξ_{SH} increases with increasing temperature can be explained by the temperature dependence of ρ_{Pt} and the magnetic proximity effect [35, 36]. In perpendicularly magnetized Pt/Co bilayers, Nguyen *et al* have reported that ξ_{SH} per unit current density is enhanced by an increase in ρ_{Pt}, which is consistent with an intrinsic SHE mechanism [35]. This effect could be used to understand our result. When the temperature increases from 50 K to 300 K, in our Pt/Co/Pt heterojunction ρ_{Pt} almost linearly increases from 47.9 $\mu\Omega$ cm to 63.3 $\mu\Omega$ cm. The increased ρ_{Pt} will induce an increase of ξ_{SH}, which is consistent with our results. Moreover, ξ_{SH} is also related to the temperature-dependent magnetic proximity effect [36]. The increase of ξ_{SH} would be also ascribed to the reduced proximity-induced magnetic moments with the increasing temperature.

In conventional quantum system, because the potential profile becomes clearer, the Rashba term corresponding to the field-like torque should increase with decreasing the temperature. This could well explain our temperature dependence of field-like torque. However, our result contrasts with the previous works, in which field-like torque increases with increasing the temperature. The opposite temperature dependence of the field-like torque is related to the interfacial current. Within the scenario of interfacial Rashba torque, the increase of field-like torque could be attributed to an increase in bulk resistance upon an increase in temperature, thereby increasing the current flowing through the interface. This enhancement can therefore be accompanied by an increase in field-like torque. Because the Rashba effect is reduced in our Pt/Co/Pt heterojunction, another possible origin of this field-like torque might be the presence of spin swapping. As suggested

in previous theories and experiments [37, 38], spin swapping will decrease with increasing temperature, leading to a decrease in field-like torque. We emphasize that this explanation remains speculative and requires further experiments to be able to confirm.

3. Conclusions

In summary, we have investigated the temperature dependence of spin–orbit torques in a Pt/Co/Pt heterojunction. Compared with the asymmetrical heterojunction, the damping-like torque of a Pt/Co/Pt heterojunction could be obviously influenced by temperature. The damping-like effective field increases with increasing temperature, indicating that the lower switching current density would be obtained under room or higher temperature. Our results highlight the Pt/Co/Pt heterojunction as a very promising class of SOT device, operating in a high temperature range.

Acknowledgments

This work is supported by the NSFC of China (Grant Nos. 11774139, 11674143), PCSIRT (Grand No. IRT-16R35) and the Program for Science and Technology of Gansu Province (Grant No. 17YF1GA024).

ORCID iDs

Shiwei Chen https://orcid.org/0000-0002-8244-1189
Li Xi https://orcid.org/0000-0003-0311-8197
Dezheng Yang https://orcid.org/0000-0001-8527-8519

References

[1] Miron M, Garello K, Gaudin G, Zermatten P J, Costache M V, Auffret S, Bandiera S, Rodmacq B, Schuhl A and Gambardella P 2011 *Nature* **476** 189
[2] Liu L, Lee O J, Gudmundsen T J, Ralph D C and Buhrman R A 2012 *Phys. Rev. Lett.* **109** 096602
[3] Emori S, Bauer U, Ahn S M, Martinez E and Beach G S 2013 *Nat. Mater.* **12** 611
[4] Ryu K S, Thomas L, Yang S H and Parkin S 2013 *Nat. Nanotechnol.* **8** 527
[5] Torrejon J, Kim J, Sinha J, Mitani S, Hayashi M, Yamanouchi M and Ohno H 2014 *Nat. Commun.* **5** 4655
[6] Awad A A, Dürrenfeld P, Houshang A, Dvornik M, Iacocca E, Dumas R K and Åkerman J 2016 *Nat. Phys.* **13** 292
[7] Liu R H, Lim W L and Urazhdin S 2015 *Phys. Rev. Lett.* **114** 137201
[8] Demidov V E, Urazhdin S, Ulrichs H, Tiberkevich V, Slavin A, Baither D, Schmitz G and Demokritov S O 2012 *Nat. Mater.* **11** 1028
[9] Hirsch J E 1999 *Phys. Rev. Lett.* **83** 1834
[10] Liu L, Pai C, Li Y, Tseng H W, Ralph D C and Buhrman R A 2012 *Science* **336** 555
[11] Dyakonov M I and Perel V I 1971 *Phys. Lett.* A **35** 459
[12] Miron I M, Gaudin G, Auffret S, Rodmacq B, Schuhl A, Pizzini S, Vogel J and Gambardella P 2010 *Nat. Mater.* **9** 230
[13] Lee K S, Lee S W, Min B C and Lee K J 2013 *Appl. Phys. Lett.* **102** 112410
[14] Emori S, Bauer U, Woo S and Beach G S D 2014 *Appl. Phys. Lett.* **105** 222401
[15] Wadley P *et al* 2016 *Science* **351** 587
[16] Kim J, Sinha J, Hayashi M, Yamanouchi M, Fukami S, Suzuki T, Mitani S and Ohno H 2013 *Nat. Mater.* **12** 240
[17] Meng K K, Miao J, Xu X G, Wu Y, Zhao X P, Zhao J H and Jiang Y 2017 *Appl. Phys. Lett.* **110** 142401
[18] Qiu X, Legrand W, He P, Wu Y, Yu J, Ramaswamy R, Manchon A and Yang H 2016 *Phys. Rev. Lett.* **117** 217206
[19] Qiu X, Narayanapillai K, Wu Y, Deorani P, Yang D H, Noh W S, Park J H, Lee K J, Lee H W and Yang H 2015 *Nat. Nanotechnol.* **10** 333
[20] Safeer C K, Jue E, Lopez A, Buda-Prejbeanu L, Auffret S, Pizzini S, Boulle O, Miron I M and Gaudin G 2016 *Nat. Nanotechnol.* **11** 143
[21] Qiu X, Deorani P, Narayanapillai K, Lee K S, Lee K J, Lee H W and Yang H 2014 *Sci. Rep.* **4** 4491
[22] Kim J, Sinha J, Mitani S, Hayashi M, Takahashi S, Maekawa S, Yamanouchi M and Ohno H 2014 *Phys. Rev.* B **89** 174424
[23] Ou Y, Pai C F, Shi S, Ralph D C and Buhrman R A 2016 *Phys. Rev.* B **94** 140414
[24] Wen Y, Wu J, Li P, Zhang Q, Zhao Y, Manchon A, Xiao J Q and Zhang X 2017 *Phys. Rev.* B **95** 104403
[25] Hayashi M, Kim J, Yamanouchi M and Ohno H 2014 *Phys. Rev.* B **89** 144425
[26] Li D, Cui B, Wang T, Yun J, Guo X, Wu K, Zuo Y, Wang J, Yang D and Xi L 2017 *Appl. Phys. Lett.* **110** 132407
[27] Garello K, Miron I M, Avci C O, Freimuth F, Mokrousov Y, Blugel S, Auffret S, Boulle O, Gaudin G and Gambardella P 2013 *Nat. Nanotechnol.* **8** 587
[28] Haney P M, Lee H W, Lee K J, Manchon A and Stiles M D 2013 *Phys. Rev.* B **87** 174411
[29] Hin Sim C, Cheng Huang J, Tran M and Eason K 2014 *Appl. Phys. Lett.* **104** 012408
[30] Liu L, Moriyama T, Ralph D C and Buhrman R A 2011 *Phys. Rev. Lett.* **106** 036601
[31] Zhang W, Han W, Jiang X, Yang S H and Parkin S S P 2015 *Nat. Phys.* **11** 496
[32] Pai C F, Ou Y, Vilela-Leão L H, Ralph D C and Buhrman R A 2015 *Phys. Rev.* B **92** 064426
[33] Hao Q and Xiao G 2015 *Phys. Rev.* B **91** 224413
[34] Ham W S, Kim S, Kim D H, Kim K J, Okuno T, Yoshikawa H, Tsukamoto A, Moriyama T and Ono T 2017 *Appl. Phys. Lett.* **110** 242405
[35] Nguyen M H, Ralph D C and Buhrman R A 2016 *Phys. Rev. Lett.* **116** 126601
[36] Zhang W, Jungfleisch M B, Jiang W, Liu Y, Pearson J E, Velthuis S G, Hoffmann A, Freimuth F and Mokrousov Y 2015 *Phys. Rev.* B **91** 115316
[37] Saidaoui H B and Manchon A 2016 *Phys. Rev. Lett.* **117** 036601
[38] Wen Y, Wu J, Li P, Zhang Q, Zhao Y, Manchon A, Xiao J Q and Zhang X 2017 *Phys. Rev.* B **95** 104406